

Conduction-electron-spin resonance in organic conductors: α and β phases of di[bis(ethylenedithio)tetrathiafulvalene]triiodide [(BEDT-TTF)₂I₃]

Tadashi Sugano, Gunzi Saito, and Minoru Kinoshita

The Institute for Solid State Physics, The University of Tokyo, Roppongi, Minato-ku, Tokyo 106, Japan

(Received 9 December 1985)

The electron-spin resonance g value, linewidth, line shape, and spin susceptibility of single crystals of the α and β phases of di[bis(ethylenedithio)tetrathiafulvalene]triiodide [(BEDT-TTF)₂I₃] are each found to show marked temperature and angular dependences in the temperature range from 5 to 300 K. In both phases, a Dysonian line-shape characteristic of conduction-electron-spin resonance is observed at room temperature when the microwave electric field is applied parallel to the quasi-two-dimensional conducting plane of the crystal. In the superconducting phase of β -(BEDT-TTF)₂I₃ with appropriate crystal size, it is found that when the microwave electric field is applied perpendicular to the plane a Lorentzian line shape observed at room temperature is gradually converted to a Dysonian line shape with decreasing temperature. These phenomena are discussed in comparison with the transport parameters derived from the reflectance spectra and the conductivity measurements. The spin diffusion constants in the α and β phases are estimated to be about 0.2 and 0.3 cm²s⁻¹, respectively. These constants are in agreement with the carrier diffusion constants evaluated independently by the analysis of the reflectance spectra. For the α phase, it is suggested from the temperature dependences of the g value and linewidth that there is a strong interaction between the triiodide and BEDT-TTF ions and the magnitude of the interaction changes suddenly with the metal-insulator transition.

I. INTRODUCTION

Bis(ethylenedithio)tetrathiafulvalene (BEDT-TTF), which is the basis of several ambient-pressure organic superconductors, has been shown to form many cation radical salts with inorganic anions, X , exhibiting wide structural and stoichiometric varieties for each anion,¹⁻³ whereas tetramethyltetraselenafulvalene (TMTSF), which also is an ambient-pressure organic superconductor, forms essentially isomorphic compounds with the unique stoichiometry of (TMTSF)₂X.⁴

Among these BEDT-TTF salts, those of the form (BEDT-TTF)_xI_y are especially interesting, because they are semiconducting or superconducting at low temperatures, while all show metallic temperature dependences for the conductivity in their high-temperature phases. To our knowledge five phases of (BEDT-TTF)_xI_y have been reported; the α phase of (BEDT-TTF)₂I₃ and δ -(BEDT-TTF)I₃ are semiconducting below 135–140 K (Refs. 5–7) and 130 K (Ref. 3), respectively, while the β phase of (BEDT-TTF)₂I₃,⁸⁻¹⁰ γ -(BEDT-TTF)₆(I₃)₅,^{3,11} and ϵ -(BEDT-TTF)₄(I₃)₂(I₈),^{3,12} are superconducting at low temperatures under ambient pressure. This remarkable polymorphism in the BEDT-TTF compounds makes it possible to carry out comparative works on the physical properties with varying stoichiometry and/or crystal structure without changing chemical components.

The electron-spin-resonance (ESR) spectra of α - and β -(BEDT-TTF)₂I₃ have very recently been reported by Azevedo *et al.*¹³⁻¹⁵ However, the reports did not give a detailed discussion of the g tensor of the crystals, the characteristic parameters of conduction-electron-spin resonance, and the nature of the phase transition occurring in the α phase. In this paper, therefore, we report the

electronic properties of the α and β phases of (BEDT-TTF)₂I₃ studied by means of ESR measurements on single crystals and discuss the spin and carrier diffusion in the crystals in comparison with the transport parameters evaluated by the analysis of the reflectance spectra reported previously.¹⁶ We also discuss the g tensors of both phases with regard to the donor molecular geometry in the crystals. Finally, we suggest that there is considerable interaction between the triiodide and the BEDT-TTF in the α phase.

II. EXPERIMENTAL DETAILS

Distorted-hexagon plate-shaped single crystals were prepared by electrochemical oxidation of BEDT-TTF in a benzonitrile solution on a platinum anode under a constant current of 1–2 μ A at room temperature. Tetra-*n*-butylammonium triiodide was used as the supporting elec-

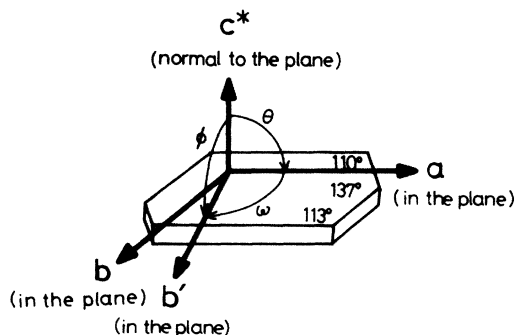


FIG. 1. Morphology and relation among directions of principal axes for the single crystal of β -(BEDT-TTF)₂I₃. The static field was rotated along the a - b' , a - c^* , and b' - c^* planes.

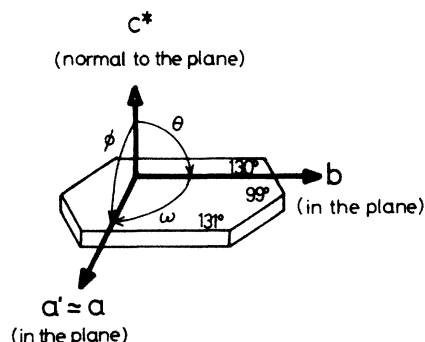


FIG. 2. Morphology and relation among directions of principal axes for the single crystal of α -(BEDT-TTF) $_2$ I $_3$. The static field was rotated along the a - b , a - c^* , and b - c^* planes.

trolyte. Both the α and β phases were crystallized in the same batch, in accordance with the result reported by Kaminskii *et al.*⁵ Either phase could easily be identified from its distinct morphology as shown in Figs. 1 and 2. Typical sample sizes were 1–2 mm in width and 0.05–0.07 mm in thickness.

ESR spectra were recorded over the temperature range 5–300 K by using a JEOL JES-FE1XG X-band (9.2 GHz) ESR spectrometer equipped with an Oxford Instruments ESR-900 continuous-flow cryostat and a DTC-2 temperature controller. The temperature was measured by using an (0.03-at. %Fe)–gold–Chromel thermocouple and controlled within ± 0.5 K. In this apparatus the resonant cavity was always kept at room temperature and hence its quality factor did not change. Therefore, it was necessary only to correct for intensity variation due to changes in the modulation width and amplification ratio in the calculation of the spin susceptibility for a signal of symmetric line shape. In the case of a Dysonian line shape, we only derived the peak-to-peak linewidth of the pure-absorption portion by assuming a linear combination of Lorentzian absorption and dispersion, and did not attempt to calculate the spin susceptibility, because it was rather difficult to estimate the skin depth with high accuracy. The sample was placed at the center of a cylindrical cavity in the TE $_{011}$ mode. The microwave magnetic field B_1 was always in the vertical direction and the static field B was in the horizontal direction. The sample was rotated around the vertical axis by using a homemade goniometer. Prior to the ESR measurements, the crystal axes were determined by measurements of reflectance spectra. The crystal was rotated around three orthogonal axes as shown in Figs. 1 and 2. The g value was determined by comparing the resonance position with that of Li $^+$ TCNQ $^-$ ($g=2.0026$). The modulation width was always kept much less than one-tenth of the linewidth to prevent distortion of line shape due to overmodulation.

III. RESULTS AND DISCUSSION

A. g value, linewidth, and line-shape anisotropy

1. β phase

The g value and the peak-to-peak linewidth are found to be anisotropic for each phase, while the intensities are

isotropic within our experimental accuracy. Figure 3 shows the angular dependence of the g value observed for β -(BEDT-TTF) $_2$ I $_3$ at 296 K. The direction of B was rotated as illustrated in Fig. 1.¹⁷ The open circles, the open triangles, and the crosses represent the g values measured by rotations of B from the c^* to the b' axis (θ), from the c^* to the a axis (φ), and from the a to b' axis (ω), respectively. The g value exhibits one maximum at 2.0103(3) (hereafter, the figure in the parentheses is the estimated standard deviation given in the last decimal place) and one minimum at 2.0026(2) for 180° rotation in the c^* - b' plane. The angular dependence of the g value is qualitatively in agreement with that reported by Venturini *et al.*¹⁵ However, the minimum g value observed by us is smaller than that reported by them. This discrepancy is not surprising because they varied the direction of B from normal to the sample plane (parallel to the c^* axis) to an arbitrary direction in the plane (the a - b plane). Therefore, the minimum g values do not necessarily coincide with each other, while the maximum g values should be nearly equal to each other as actually observed. Since the reported minimum g value of 2.0042(1) is an intermediate between minimum g values observed for c^* - b' [$g=2.0026(2)$] and c^* - a [$g=2.0059(2)$] rotations in our experiments, the field direction in the a - b plane employed by them would fall between the a and b' axis, being near the middle of these axes.

The angular dependence of g value of the crystal is well interpreted by taking into account the principal values and axes of the g tensor of the BEDT-TTF cation radical and the manner of the molecular stacking of BEDT-TTF in the crystal. To determine the principal values and axes of the g tensor, we carried out a least-squares fitting to the equation

$$g^2 = \sum_{i,j=1}^n g_{ij}^2 l_i l_j, \quad (1)$$

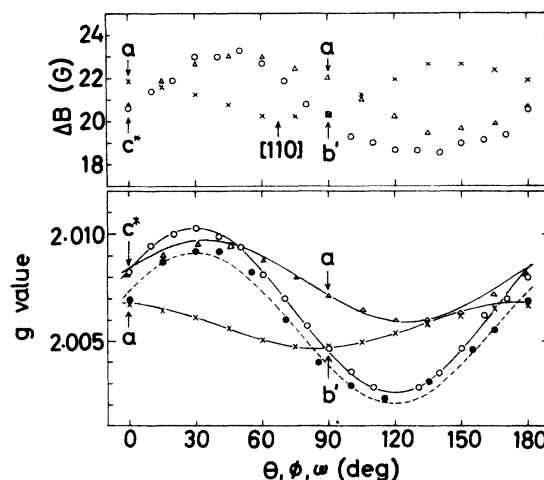


FIG. 3. Angular dependence of g value and peak-to-peak linewidth ΔB for β -(BEDT-TTF) $_2$ I $_3$; open circles, open triangles, and crosses represent the data obtained at 296 K by c^* - b' , c^* - a , and a - b' rotations, respectively. Calculated g values for each rotation are shown by solid lines. Angular dependence of g value in the c^* - b' plane at 5 K is also shown by solid circles.

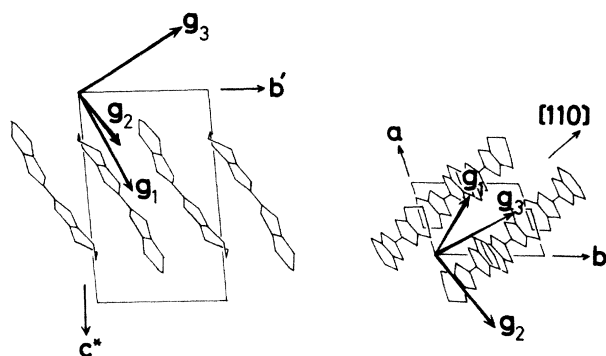


FIG. 4. Relation between the directions of the principal axes of the g tensor and crystal structure of β -(BEDT-TTF) $_2$ I $_3$. Note that g_1 , g_2 , and g_3 are oriented approximately parallel to the long, short axes of the BEDT-TTF molecule and perpendicular to the molecular plane, respectively.

where l is the direction cosine of principal axis. The g values calculated are shown by solid lines in Fig. 3 and are found to be in good agreement with the g values observed. The directions of the principal axes of the g tensor in the crystal thus obtained are shown in Fig. 4. It is clearly seen that the directions of $g_1=2.0111(2)$, $g_2=2.0065(2)$, and $g_3=2.0025(2)$ are nearly parallel to the molecular long axis, the short axis, and the direction normal to the molecular plane of BEDT-TTF, respectively. The principal values of the molecular g tensor of TTF derivatives are known to be $g_1=2.011-2.014$, $g_2=2.006-2.009$, and $g_3=2.002-2.003$ for the directions of molecular long axis, short axis, and normal to the molecular plane, respectively.¹⁸ Furthermore, an average of the principal g values ($\bar{g}=2.0067$) observed for β -(BEDT-TTF) $_2$ I $_3$ is almost equal to the g value of the BEDT-TTF $^+$ radical in solution ($g=2.0073$), as listed in Table I. These results suggest that the g values of the crystal of β -(BEDT-TTF) $_2$ I $_3$ are essentially determined by the g tensor of the BEDT-TTF cation radical.

The g value anisotropy in the c^*-b' plane at 5 K shown by the solid circles in Fig. 3 is qualitatively similar to that at 296 K. A maximum of 2.0094(2) and a minimum of 2.0024(2) are smaller to some extent than those at 296 K. The maximum g value in the $a-b$ (i.e., $a-b'$) plane at 10 K is reported to be 2.00750(5) and the minimum is 2.00435(5).¹⁵ These values are very close to the g values of 2.0068(2) and 2.0046(2) observed at 296 K by us. Al-

though the local displacement of BEDT-TTF molecule and triiodide ion occurs below 200 K,¹⁹ the g tensor of β -(BEDT-TTF) $_2$ I $_3$ at 5 K is not very much different from that at room temperature.

Figure 3 also shows the angular dependence of the peak-to-peak linewidth ΔB observed for β -(BEDT-TTF) $_2$ I $_3$ at 296 K. In our crystals, a Dysonian line-shape characteristic of conduction-electron-spin resonance was observed only when B was rotated from the a axis to the b' axis, i.e., in the $a-b$ plane. Therefore, ΔB of the pure-absorption portion of the Dysonian signal is shown for this case. On the other hand, Venturini *et al.*¹⁵ observed the Dysonian line shape when B was normal to the plane. The reason why the Dysonian line shape was observed here solely when B was in the $a-b$ plane will be discussed later, together with the temperature dependence of line shape.

The angular dependence of ΔB is somewhat different from that of g value. First, the directions exhibiting maximum and minimum ΔB do not coincide with those giving the maximum and minimum g values. Second, the anisotropic part of ΔB is not simply proportional to the square of $\Delta g = g - 2.0023$. These would imply that Elliott's relationship between ΔB and the g value for the anisotropic case^{20,21} is not directly applicable to the interpretation of the angular dependence of linewidth for β -(BEDT-TTF) $_2$ I $_3$.

2. α phase

Figure 5 shows the angular dependence of the g value observed for α -(BEDT-TTF) $_2$ I $_3$ at 296 K. The direction of B was rotated as illustrated in Fig. 2.²² The open circles, open triangles, and crosses represent the g values measured by rotation of B from the c^* to the b axis (θ), from the c^* to the a' axis (φ), and from the b to the a' axis (ω), respectively. The g -value anisotropy for c^*-b rotation is quite similar to that for c^*-a' rotation within the experimental errors, while the g value is almost isotropic for the $b-a'$ rotation. These results suggest that the g tensor of α -(BEDT-TTF) $_2$ I $_3$ is axially symmetric around the c^* axis of crystal.

The g -value anisotropy of α -(BEDT-TTF) $_2$ I $_3$ is also well interpreted in terms of the g tensor of the BEDT-TTF cation radical. The principal values and axes of g tensor of α -(BEDT-TTF) $_2$ I $_3$ were determined by least-squares fitting to Eq. (1). Since the g tensor of crystal is axially symmetric, only $g_1=2.0113(3)$ is obtained. The

TABLE I. Principal values of the g tensor for some BEDT-TTF compounds at room temperature.

Compound	\bar{g}	g_1	g_2	g_3
α -(BEDT-TTF) $_2$ I $_3$	2.0060	2.0113	2.0033	
β -(BEDT-TTF) $_2$ I $_3$	2.0067	2.0111	2.0065	2.0025
(BEDT-TTF) $_2$ SbF $_6^a$	2.0070	2.0115	2.0070	2.0026
(BEDT-TTF) $_2$ AsF $_6^a$	2.0069	2.0116	2.0067	2.0023
BEDT-TTF $^+$ in PhCN b	2.00737			
BEDT-TTF $^+$ in TCE c	2.00734			

^aReference 23.

^bBenzonitrile.

^c1,1,2-trichloroethane.

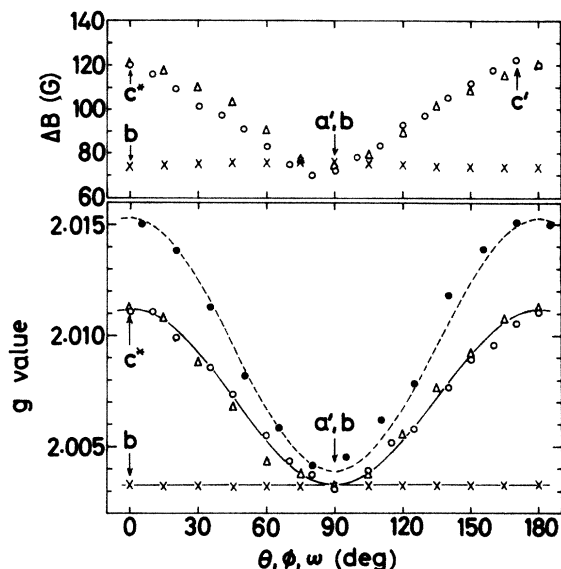


FIG. 5. Angular dependence of g value and peak-to-peak linewidth ΔB for α -(BEDT-TTF) $_2$ I $_3$; open circles, open triangles, and crosses represent the data obtained at 296 K by c^* - a' , c^* - b , and a' - b rotations, respectively. Calculated g values are shown by solid lines. Angular dependence of the g value in the c^* - a' plane at 5 K is also shown by solid circles.

values of g_2 and g_3 are averaged at 2.0033(3) in the a - b plane. The principal value g_1 obtained for α -(BEDT-TTF) $_2$ I $_3$ is in good agreement with that of β -(BEDT-TTF) $_2$ I $_3$, (BEDT-TTF) $_2$ SbF $_6$,²³ and (BEDT-TTF) $_2$ AsF $_6$,²³ as summarized in Table I, and the direction of its principal axis is found to be nearly parallel to the c^* axis. In the α phase, the long axis of the BEDT-TTF species is approximately parallel to the c^* axis as shown in Fig. 6, while there are large dihedral angles between their molecular planes, 59.4(5)° and 70.4(5)°.²² Therefore, the direction of g_1 is nearly parallel to the molecular long axis of the BEDT-TTF species. This is strikingly similar to the result obtained for β -(BEDT-TTF) $_2$ I $_3$.

The nearly isotropic nature of the g value in the a - b plane of α -(BEDT-TTF) $_2$ I $_3$ is possibly due to zigzag orientations²² of BEDT-TTF species along the plane. As mentioned above, g_1 is essentially determined by the g_1 of BEDT-TTF species because of approximately parallel

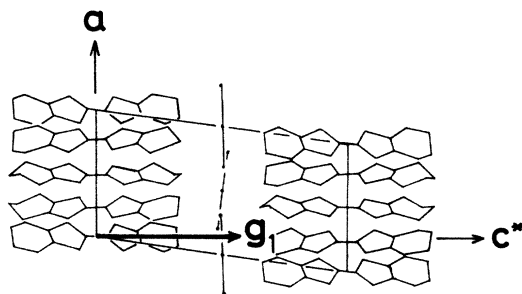


FIG. 6. Relation between the directions of principal axes of g tensor and crystal structure of α -(BEDT-TTF) $_2$ I $_3$. Note that that g_1 is oriented parallel to the long axis of the BEDT-TTF molecule.

alignment of the long axis of BEDT-TTF in the crystal. On the other hand, there are the magnetically inequivalent stacks due to the different orientations of molecular plane of BEDT-TTF. In this situation, ESR absorption would split into three lines, if the exchange interaction between the stacks is not so strong as to average out the absorptions due to the inequivalent stacks. However, only a single absorption line is observed in the whole temperature range examined here. This indicates that there is an exchange coupling between the stacks. Then, the variation of g value as a function of rotation angle may be described by an average of g values of BEDT-TTF species in the unit cell. The molecular planes of four crystallographically independent BEDT-TTF species are tilted from the b axis by approximately -35° , -35° , 28° , and 40° .²² In the a - b plane, the g value of BEDT-TTF species is mainly governed by g_2 and g_3 . We calculated g values for a rotation of B in the a - b plane in terms of an average of g values of the four magnetically inequivalent BEDT-TTF species in the unit cell. The result indicates that the g value calculated is only slightly varying with a maximum value of 2.0052 near the b axis and a minimum of 2.0038 near the a' axis. These values are somewhat larger than those observed for α -(BEDT-TTF) $_2$ I $_3$. However, the nearly isotropic nature is well reproduced by this averaging. A discrepancy between observed and calculated values would be due to the roughness of the approximation and the contribution from the triiodide ions described below.

It is to be noted that there seems to be no charge separation or mixed-valent nature of the BEDT-TTF species in the α phase. If there is charge separation, as suggested by Mori *et al.*,²⁴ the g -value anisotropy in the a - b plane would have to be greatly enhanced. Based on the molecular structure reported by Bender *et al.*,²² they have suggested that two of the four crystallographically independent BEDT-TTF species tilted from the b axis by -35° are fully ionized, while the other two, tilted by 28° and 40° , are neutral. Then, only the former two species might contribute to the g -value anisotropy. In this case, the g value would vary from 2.0025 to 2.0065, contrary to our observation. Very recently, Leung *et al.* also claimed that the independent BEDT-TTF molecules in the unit cell are chemically equivalent.²⁵

The g -value anisotropy in the c^* - a' plane at 5 K shown by solid circles in Fig. 5 is remarkably different from that at 296 K. A maximum of 2.0153(3) and a minimum of 2.0039(3) are both larger than those at 296 K and anisotropy is greatly enhanced. Nevertheless, the direction showing the maximum still remains parallel to the c^* axis. This indicates that the most prominent change in g value is related to the interaction along the c^* axis. It is shown that two-dimensional sheets of BEDT-TTF are interleaved by a sheet of triiodide anions and the direction perpendicular to the sheets is nearly parallel to the c^* axis.²² These facts would imply that there is an interaction of the triiodide with BEDT-TTF, because strong spin-orbit coupling of iodine atoms may cause a g value larger than that of the BEDT-TTF cation radical.

The angular dependence of the linewidth ΔB observed for α -(BEDT-TTF) $_2$ I $_3$ at 296 K is qualitatively similar to

that of the g value, as shown in Fig. 5. For our crystals, the Dysonian line shape was observed when B was rotated in the a - b plane, contrary to the result reported by Venturini *et al.*¹⁵ Therefore, when the Dysonian signal is observed, ΔB of the pure-absorption portion of the signal is given in Fig. 5. For the measurements with B normal to the plane (along the c^* axis) and the microwave magnetic field in the plane, the ESR line shape has no dispersive component (pure Lorentzian absorption), being in good agreement with the result reported.¹⁵

α -(BEDT-TTF)₂I₃ shows an extremely broad ESR signal, the maximum linewidth at room temperature being as large as 123 G (1 G = 10⁻⁴ V s m⁻²). This would also be due to the strong spin-orbit coupling caused by the interaction of the triiodide with BEDT-TTF. The above fact, together with the large g value at low temperature, indicates that there is considerable interaction of the triiodide with BEDT-TTF.

We found that ESR linewidths of α - and β -(BEDT-TTF)₂IBr₂ at room temperature are 60–70 and 17–20 G, respectively.²⁶ The narrower linewidth in the dibromiodate (IBr₂) salts is probably due more to the weaker spin-orbit coupling of bromine than it is to the coupling of iodine. Note that the room-temperature linewidth for α -(BEDT-TTF)₂I₃ is 4–6 times as large as that for β -(BEDT-TTF)₂I₃. A similar relation is also observed for the two phases of IBr₂ salt. Therefore, the interaction between trihalide ions and BEDT-TTF species is stronger in the α phase than in the β phase. Therefore, the strength of the interaction seems to be mainly related to the difference in crystal structure, although the two α phases are not strictly isostructures.^{25,27}

B. Spin and charge diffusion in the metallic phase

In the highly conducting phase, the α and β phases of (BEDT-TTF)₂I₃ exhibit the Dysonian line shape when the microwave electric field is applied parallel to the quasi-two-dimensional conducting plane (i.e., the a - b plane). The sample and field geometry for this case is shown in Figs. 7(a) and 7(c). B is rotated in the y - z plane and B_1 is always perpendicular to the plane. Therefore, the microwave electric field E perpendicular to B_1 is always parallel to the plane. The penetration of the electromagnetic waves with z polarization is determined by the conductivity σ_z and the penetration with y polarization is determined by σ_y . Hence the skin depth δ for propagation in the plane direction is determined by the equations

$$\delta_y = \left[\frac{2}{\mu_0 \sigma_y \omega} \right]^{1/2} \quad (2a)$$

and

$$\delta_z = \left[\frac{2}{\mu_0 \sigma_z \omega} \right]^{1/2}, \quad (2b)$$

where μ_0 is the permeability of free space and ω (rad s⁻¹) is the angular frequency of microwaves.

Conductivity measurements suggest that both phases have nearly isotropic charge-transport properties in the a - b plane at low frequencies. At room temperature, σ 's

of α and β phases are reported to be 60–250 (Ref. 6) and 30 (Ref. 8) S cm⁻¹, respectively. Consequently, the classical skin depth δ is estimated to be about 0.1 mm for wave propagation along the plane from Eqs. (2a) and (2b). Dyson²⁸ has shown that there are two different skin effects: one is the classical (normal) skin effect, where field penetration is controlled by δ , and the other is the

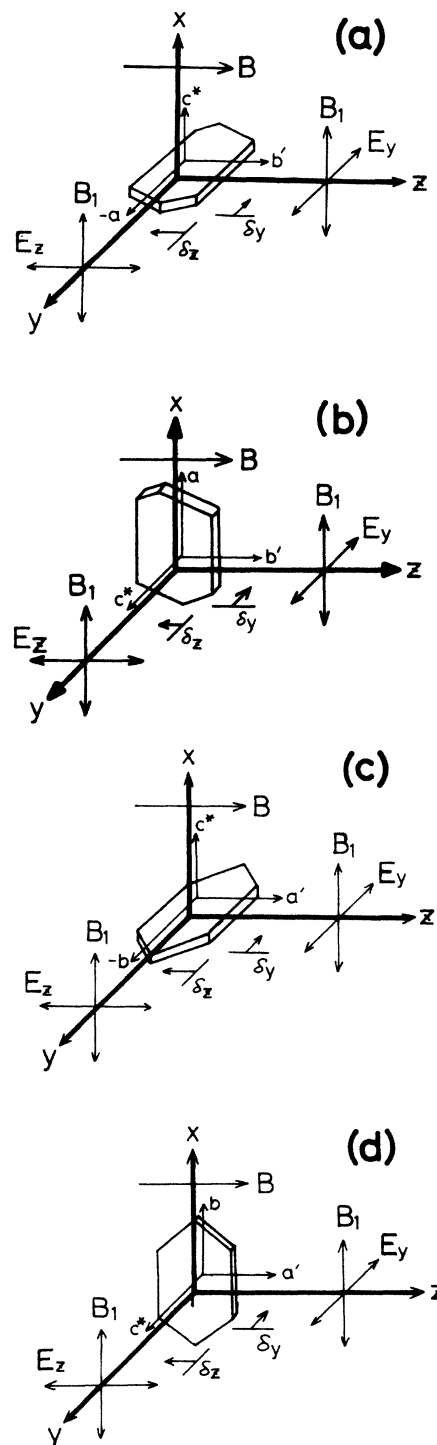


FIG. 7. Sample and field geometries used in the discussion of Dysonian line shape; (a) and (b) are for β -(BEDT-TTF)₂I₃ and (c) and (d) are for α -(BEDT-TTF)₂I₃.

anomalous skin effect, where the penetration is controlled by the mean free path Λ of carriers. From the measurements of reflectance spectra, we have previously shown that Λ 's of both phases of $(\text{BEDT-TTF})_2\text{I}_3$ are 4–7 Å (Ref. 16) at room temperature. Therefore, there is a relation $\delta \gg \Lambda$, which induces the normal skin effect. This means that the change in penetration depth is controlled by the variation of skin depth. The size of crystal plane used here is $0.6 \times 2 \text{ mm}^2$ for the β phase and $1 \times 2 \text{ mm}^2$ for the α phase. Thus the penetration depth is smaller than the crystal size even at room temperature. As the temperature is lowered, δ becomes much shorter as a result of the increase of σ .

In contrast to the results mentioned above, both phases exhibit the Lorentzian line shape at room temperature when the microwave electric field is applied not parallel to the quasi-two-dimensional plane. The sample and field geometry for this case are shown in Figs. 7(b) and 7(d). In this situation, the skin depths δ_y and δ_z are estimated with σ_z and σ_y , respectively, by using Eqs. (2a) and (2b). Taking $\sigma_z \sim 10^2 \text{ S cm}^{-1}$ and $\sigma_y \sim 10^{-1} \text{ S cm}^{-1}$ (upper limits of room-temperature values for both phases), we obtain $\delta_y \sim 60 \text{ } \mu\text{m}$ and $\delta_z \sim 1.5 \text{ mm}$. The skin depths estimated are comparable with or slightly larger than the sizes of crystal employed here, $d_y = 50\text{--}70 \text{ } \mu\text{m}$ and $d_z = 0.6\text{--}1 \text{ mm}$. Therefore, no skin effect is expected for this case.

As the temperature is lowered, δ , and hence the penetration depth of the electromagnetic waves, become smaller than the size of the crystal of β -(BEDT-TTF) $_2\text{I}_3$ because of an increase of σ . The Dysonian line shape is characterized by a ratio A/B between the maximum and minimum of the derivative of ESR absorption shown in the inset of Fig. 8. Below about 200 K, as shown in Fig. 8, A/B increases to a small extent from unity characteristic of the Lorentzian line shape. Below 100 K, A/B increases more and reaches a constant value of 2.6–2.8. In the β phase, σ increases continuously down to about 2 K by 1000 times σ at room temperature.²⁹ From the temperature variation of σ in the β phase, δ_y at 100 and 200 K can be roughly estimated to be 17 and 37 μm , respectively. This indicates that the electromagnetic waves begin to penetrate incompletely into the crystal between 100 and 200 K, and a significant skin effect is expected below about 100 K. This estimation is qualitatively in agreement with the result observed here. On the other hand, in the α phase, σ increases only by a factor of 2–3 from 300 K down to 135 K, where a metal-insulator transition occurs.^{5–7} Consequently, the penetration depth remains comparable to the crystal size. In fact, we could not observe the Dysonian line shape with the crystal of the phase for the geometry of Fig. 7(d) in the whole temperature range examined.

The time T_D that it takes an electron to diffuse through the skin depth δ is determined by the equations³⁰

$$T_{D_y} = \frac{\delta_y^2}{D_y} = \frac{2ne^2}{\mu_0\sigma_z\sigma_y\omega W_y} \quad (3a)$$

and

$$T_{D_z} = \frac{\delta_z^2}{D_z} = \frac{2ne^2}{\mu_0\sigma_z\sigma_y\omega W_z} \quad (3b)$$

where n is the density of conduction electrons, e is the elementary charge, D is the diffusion constant, and W is the bandwidth for each direction of propagation. The bandwidth $W||b$ of α -(BEDT-TTF) $_2\text{I}_3$ in the quasi-two-dimensional conducting plane is estimated to be 0.44 eV ($1 \text{ eV} = 1.602 \times 10^{-19} \text{ J}$) from the analysis of reflectance spectra¹⁶ and 0.35 eV from the theoretical calculation.²⁴ W can also be evaluated from the temperature dependence of thermopower S by using the equation for the $\frac{3}{4}$ -filled band,³¹

$$\frac{dS}{dT} = \frac{2\pi^2 k_B^2}{3eW} \quad (4)$$

where k_B is the Boltzmann constant. We estimated W for the directions parallel to the a and b axes in the plane by referring to the results reported by Merzhanov *et al.*³² $W||b \sim 0.49 \text{ eV}$ and $W||a \sim 0.22 \text{ eV}$.³³ Since these values are approximately equal to each other, we take $W_z = W||b = 0.5 \text{ eV}$, $\sigma_z = \sigma||b = 10^2 \text{ S cm}^{-1}$, and $\sigma_y = \sigma||c^* = 10^{-1} \text{ S cm}^{-1}$ for the sample and field geometry shown in Fig. 7(c). Then, $T_{D_z} = 0.12 \text{ s}$. The minimum ESR linewidth observed for the geometry ($\Delta B||b$) is 70 G. Thus, $T_2 < 10^{-8} \text{ s}$. Therefore, we conclude that the condition $T_D \gg T_2$ is well satisfied over the entire temperature range of measurements.

The diffusion constant D_z for the spin propagation along the b axis in the conducting plane may also be evaluated by Eq. (3b). Taking $\delta_z = 1.5 \text{ mm}$, we obtain $D_z = 0.2 \text{ cm}^2 \text{ s}^{-1}$. The carrier diffusion constant can be derived independently from the equation

$$D = v_F^2 \tau \quad (5)$$

where v_F is the Fermi velocity and τ is the relaxation time of carriers. These quantities have already been evaluated from the Drude analysis of reflectance spectra:¹⁶ $v_F = 1.8 \times 10^5 \text{ m s}^{-1}$ and $\tau = 2.4 \times 10^{-15} \text{ s}$. Then, $D = 0.78 \text{ cm}^2 \text{ s}^{-1}$. This value roughly agrees with D_z .

The same analysis is also applicable to β -(BEDT-TTF) $_2\text{I}_3$ for the field geometry shown in Fig. 7(a). The bandwidth $W||[110]$ is estimated to be 0.52–0.66 eV from the Drude analyses of reflectance spectra,^{16,34} 0.5 eV from the theoretical calculation,²⁴ and 0.48 eV from the temperature dependence of the thermopower.³¹ Since these values are approximately equal to each other and $W||b \sim W||[110]$, we take $W_z = W||b = 0.6 \text{ eV}$, $\sigma_z = \sigma||b = 10^2 \text{ S cm}^{-1}$, and $\sigma_y = \sigma||c^* = 10^{-1} \text{ S cm}^{-1}$. Then, $T_{D_z} = 0.08 \text{ s}$. Again, the condition $T_D \gg T_2$ is well satisfied, because $T_2 \sim 10^{-7} \text{ s}$ is estimated from the minimum linewidth of 5 G. Taking $\delta_z = 1.5 \text{ mm}$, we obtain $D_z = 0.3 \text{ cm}^2 \text{ s}^{-1}$. This agrees with $D = 1.5 \text{ cm}^2 \text{ s}^{-1}$ derived from the values $v_F = 2.3 \times 10^5 \text{ m s}^{-1}$ and $\tau = 2.8 \times 10^{-15} \text{ s}$, which have been obtained by the Drude analysis of reflectance spectra.¹⁶ Under the condition $T_D \gg T_2$, the ratio A/B should approach 2.7.³⁵ The values of A/B at low temperatures are found to be 2.6–2.8. Therefore, the condition $T_D \gg T_2$ is also supported by the line shape at low temperatures.

As mentioned above, the temperature and angular variations of the ESR line shape observed for the highly conducting phase of α - and β -(BEDT-TTF) $_2\text{I}_3$ are well

described in terms of Dyson's skin-depth theory. The skin depth δ is found to be much larger than the electron mean free path Λ , and the spin-diffusion time T_D is also evaluated to be very much larger than the spin-spin relaxation time T_2 . Under the conditions $\delta \gg \Lambda$ and $T_D \gg T_2$, the ratio A/B characteristic of Dysonian line shape is predicted to be 2.7,³⁵ which is actually observed for β -(BEDT-TTF)₂I₃ at low temperatures. The spin-diffusion constant obtained from the results of ESR measurements essentially agrees with the carrier diffusion constant evaluated independently from the analysis of reflectance spectra. This fact, together with the fact that the ESR line shape is well described in terms of Dyson's theory, is consistent with the metallic behavior of conductivity observed for α - and β -(BEDT-TTF)₂I₃.

C. Temperature dependence of g value, linewidth, and spin susceptibility

Figure 8 shows the temperature dependence of ΔB for the crystals of β -(BEDT-TTF)₂I₃ measured with the field and sample geometry shown in Fig. 7(b) (i.e., $B \parallel b'$ and $B_1 \parallel a$). The linewidth at low temperature is the peak-to-peak linewidth of the pure-absorption portion of the measured Dysonian signal. The linewidth increases approximately linearly with increasing temperature up to 300 K, although a slight change in slope appears around 150 K. This behavior is in good agreement with that of ΔB measured with a different field geometry, $B \parallel c^*$ and $B_1 \parallel (001)$.¹⁵ Furthermore, the values of ΔB measured with both geometries coincide well with each other, as shown in Fig. 8. Therefore, the temperature dependence of ΔB in β -(BEDT-TTF)₂I₃ seems to be isotropic in the whole temperature range 10–300 K.

A linear broadening of ΔB with increasing temperature is expected when the spin-lattice relaxation of conduction-electron spin in metal is dominated by modulation of spin-orbit coupling by lattice vibrations, if the direct (one-phonon) process is assumed.³⁶ The nearly isotropic and linear temperature dependence observed is con-

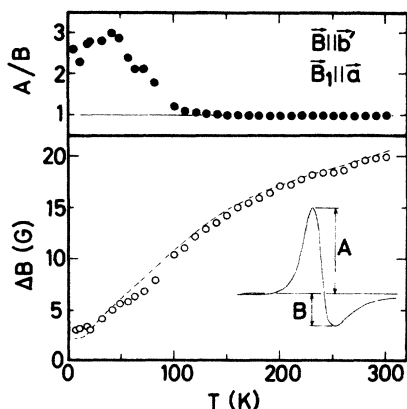


FIG. 8. Temperature dependence of peak-to-peak linewidth ΔB and ratio A/B between the maximum and minimum of the derivative of absorption (see inset) for β -(BEDT-TTF)₂I₃. The result reported in Ref. 15 with different field geometry ($B \parallel c^*$) is shown by the dashed line.

sistent with this relaxation mechanism. Therefore, it is concluded that β -(BEDT-TTF)₂I₃ has metallic character in spite of the relatively low conductivity⁵ at room temperature as an organic conductor.

In Fig. 9 the temperature dependence of the g value and linewidth, and the spin susceptibility, for the single crystal of α -(BEDT-TTF)₂I₃, is shown. These data were taken with the geometry of $B \parallel c^*$ and $B_1 \parallel b$, for which the temperature variations of g value and linewidth were most prominent. A significant feature is the shift of g value toward the larger- g -value side with decreasing temperature. As shown in Fig. 9, the g value increases gradually from 2.0113(3) at 296 K with decreasing temperature and exhibits a sharp maximum of 2.0167(3) just above the metal-insulator-transition temperature 140 K. Below 140 K, the g value becomes temperature independent with $g=2.0151(2)$. These g values are considerably larger than those observed for other BEDT-TTF cation radical salts and free BEDT-TTF⁺ ions in solution. As described in the preceding section, the g -value shift is caused by the interaction between the triiodide and BEDT-TTF. From the temperature variation of the g value, therefore, it is suggested that, in the high-temperature (metallic) phase, the interaction becomes stronger with decreasing temperature. In the low-temperature (semiconductive) phase, the interaction becomes independent of temperature and there still remains considerably strong interaction. At the phase-transition temperature, the strength of the interaction changes discontinuously. As suggested in the preceding section, the strength of the interaction seems to be related to the difference in the crystal structure. Therefore, the discontinuous change of g value implies that the metal-insulator transition is incorporated with a structural change in α -(BEDT-TTF)₂I₃, although crystal structure at low temperature has not yet been fully determined.³⁷

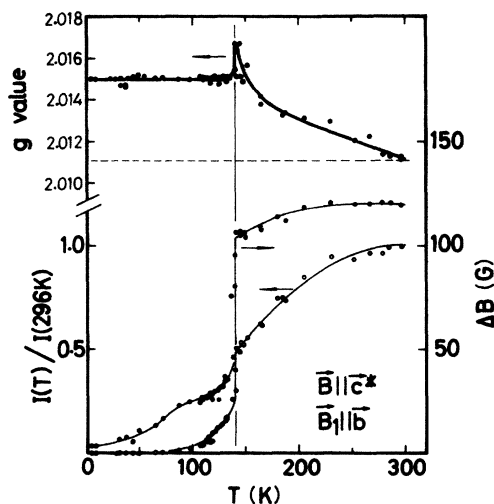


FIG. 9. Temperature dependence of g value, peak-to-peak linewidth ΔB , and spin susceptibility I for α -(BEDT-TTF)₂I₃. The solid lines are guides to the eye and the dashed line represents g_1 for β -(BEDT-TTF)₂I₃ at 296 K. The discontinuous decrease near 140 K agrees well with a similar decrease in conductivity.

The spin susceptibility in the metallic phase decreases gradually with decreasing temperature, contrary to the slight increase observed by Venturini *et al.*¹⁵ Merzhanov *et al.*³² have also shown that the static susceptibility decreases with decreasing temperature. At 140 K the spin susceptibility I decreases discontinuously by a factor of 2 and, below 130 K, it can be fitted to an exponential equation of the form

$$I = (C/T) \exp(-J/k_B T), \quad (6)$$

where $J = 0.042$ eV. This behavior is also in agreement with that of static susceptibility with $J = 700$ K (0.06 eV).³²

The peak-to-peak linewidth ΔB is almost constant between 200 and 300 K. This behavior agrees qualitatively with the result reported.¹⁵ However, the linewidth observed here (120 G) is a little larger than that reported (95 G), although the experimental geometries are similar to each other.

The temperature dependence of the linewidth in the metallic phase of α -(BEDT-TTF)₂I₃ is very different from that of β -(BEDT-TTF)₂I₃. This difference would be interpreted in terms of the interaction between the triiodide and BEDT-TTF. We have previously shown that there is a magnetic interaction between the TTF⁺ radical and iodine atom in TTF-I_{0.71}.³⁸ The average g value ($\bar{g} = 2.013$) of TTF-I_{0.71} is large in comparison with that of the TTF⁺ ion in solution ($g = 2.00838$) and ΔB is very large (180 G) at 300 K. These values are similar to those of α -(BEDT-TTF)₂I₃. On the other hand, in the metallic phase of TTF-I_{0.71} above 210 K, \bar{g} is constant and ΔB changes linearly with temperature.³⁸ The temperature dependence of ΔB of TTF-I_{0.71} is rather similar to that observed for β -(BEDT-TTF)₂I₃, although there is considerably strong interaction between iodine and TTF⁺. Thus, ΔB for the metallic phase seems to change linearly with temperature, if the g value and hence the interaction between iodine and the cation radical is insensitive to temperature. Nevertheless, this does not hold for the metallic phase of α -(BEDT-TTF)₂I₃ in which ΔB is nearly constant and \bar{g} changes with temperature. In α -(BEDT-TTF)₂I₃, it is therefore suggested that the line-broadening effect expected for the metallic phase is possibly compensated by the line-narrowing effect due to the decrease of

the interaction. The apparent linewidth thus becomes nearly independent of temperature.

IV. SUMMARY AND CONCLUSIONS

The organic conductors, α - and β -phase (BEDT-TTF)₂I₃, have been found to exhibit metallic behavior characterized by the Dysonian line shape in electron-spin resonance. The spin-diffusion constants of both phases are estimated to be about $0.2 \text{ cm}^2 \text{ s}^{-1}$ for the α phase and $0.3 \text{ cm}^2 \text{ s}^{-1}$ for the β phase from the skin depth obtained by analyzing the temperature and angular dependences of the line shape, together with the mean free path and the bandwidth, which are derived from reflectance spectra. These values are essentially in agreement with the carrier diffusion constants estimated independently from the analysis of reflectance spectra. This is also consistent with the metallic character of both phases.

The g tensors observed for the crystals of both phases are well reproduced with the molecular g tensor of the BEDT-TTF⁺ radical. This suggests that there remains molecular character, while the transport properties can be essentially explained by the Drude model valid for simple metals.

There are some very distinct differences in the details of ESR between the two phases. In the metallic region of the α phase, the ESR linewidth is extremely broad and approximately independent of temperature, while, in the β phase, it shows almost linear temperature dependence consistent with the metallic behavior. The broad linewidth, together with a larger g value than that of the BEDT-TTF⁺ radical, indicates that there is considerably strong interaction between the triiodide and BEDT-TTF⁺ in the α phase. From the temperature variations of the g value and linewidth in the α phase, we suggest that the interaction increases gradually with decreasing temperature from 300 to 140 K and decreases discontinuously at 140 K, where the metal-insulator transition occurs. In this respect, it is of great interest to elucidate the crystal structure of α -(BEDT-TTF)₂I₃ at low temperatures.

ACKNOWLEDGMENTS

This work was supported by a Grant-in-Aid for Scientific Research from the Ministry of Education, Science and Culture, Japan.

¹H. Kobayashi, R. Kato, T. Mori, A. Kobayashi, Y. Sasaki, G. Saito, T. Enoki, and H. Inokuchi, *Mol. Cryst. Liq. Cryst.* **107**, 33 (1984).

²S. S. P. Parkin, E. M. Engler, V. Y. Lee, and R. R. Schumaker, *Mol. Cryst. Liq. Cryst.* **119**, 375 (1985).

³R. P. Shibaeva, V. F. Kaminskii, and E. B. Yagubskii, *Mol. Cryst. Liq. Cryst.* **119**, 361 (1985).

⁴See, for example, J. Friedel and D. Jerome, *Contemp. Phys.* **23**, 583 (1982).

⁵V. F. Kaminskii, T. G. Prokhorova, R. P. Shibaeva, and E. B. Yagubskii, *Pis'ma Zh. Eksp. Teor. Fiz.* **39**, 15 (1984).

⁶K. Bender, K. Dietz, H. Endres, H. V. Helberg, I. Hennig, H. J. Keller, H. V. Schafer, and D. Schweitzer, *Mol. Cryst. Liq. Cryst.* **107**, 45 (1984).

⁷E. B. Yagubskii, I. F. Shchegolev, V. N. Laukhin, R. P. Shibaeva, E. E. Kostyuchenko, A. G. Khomenko, Yu. V. Sushko, and A. V. Zvarykina, *Pis'ma Zh. Eksp. Teor. Fiz.* **40**, 387 (1984).

⁸E. B. Yagubskii, I. F. Shchegolev, V. N. Laukhin, P. A. Kononovich, M. V. Karatsovnik, A. V. Zvarykina, and L. I. Buravov, *Pis'ma Zh. Eksp. Teor. Fiz.* **39**, 12 (1984).

⁹G. W. Crabtree, K. D. Carlson, L. N. Hall, P. T. Copps, H. H. Wang, T. J. Emge, M. A. Beno, and J. M. Williams, *Phys. Rev. B* **30**, 2958 (1984).

¹⁰V. B. Ginodman, A. V. Gudenko, L. N. Zherikhina, *Pis'ma Zh. Eksp. Teor. Fiz.* **41**, 41 (1985).

¹¹E. B. Yagubskii, I. F. Shchegolev, S. I. Pesotskii, V. N. Laukhin, P. A. Kononovich, M. V. Kartsovnik, and A. V. Zvarykina, *Pis'ma Zh. Eksp. Teor. Fiz.* **39**, 275 (1984).

¹²V. A. Merzhanov, E. E. Kostyuchenko, V. N. Laukhin, R. M.

- Lobkovskaya, M. K. Makova, R. P. Shibaeva, I. F. Shchegolev, and E. B. Yagubskii, *Pis'ma Zh. Eksp. Teor. Fiz.* **41**, 146 (1985).
- ¹³L. V. Azevedo, E. L. Venturini, J. E. Shirber, J. M. Williams, H. H. Wang, and T. J. Emge, *Mol. Cryst. Liq. Cryst.* **119**, 389 (1985).
- ¹⁴L. J. Azevedo, E. L. Venturini, J. F. Kwak, J. E. Shirber, J. M. Williams, H. H. Wang, and P. E. Reed, *Mol. Cryst. Liq. Cryst.* **125**, 169 (1985).
- ¹⁵E. L. Venturini, L. J. Azevedo, J. E. Shirber, J. M. Williams, and H. H. Wang, *Phys. Rev. B* **32**, 2819 (1985).
- ¹⁶T. Sugano, K. Yamada, G. Saito, and M. Kinoshita, *Solid State Commun.* **55**, 137 (1985).
- ¹⁷In this work, we refer to the crystal data given in J. M. Williams, T. J. Emge, H. H. Wang, M. A. Beno, R. T. Copps, L. N. Hall, K. D. Carlson, and G. W. Crabtree, *Inorg. Chem.* **23**, 2560 (1984).
- ¹⁸W. M. Walsh, Jr., L. W. Rupp, Jr., F. Wudl, M. L. Kaplan, D. E. Shafer, G. A. Thomas, and R. Gemmer, *Solid State Commun.* **33**, 413 (1980).
- ¹⁹P. C. W. Leung, T. J. Emge, M. A. Beno, H. H. Wang, and J. M. Williams, *J. Am. Chem. Soc.* **106**, 7644 (1984).
- ²⁰R. J. Elliott, *Phys. Rev.* **96**, 266 (1954).
- ²¹H. J. Pedersen, J. C. Scott, and K. Bechgaard, *Solid State Commun.* **35**, 207 (1980).
- ²²K. Bender, I. Hennig, D. Schweitzer, K. Dietz, H. Endres, and H. J. Keller, *Mol. Cryst. Liq. Cryst.* **108**, 359 (1984).
- ²³R. Laversanne, J. Amiel, P. Delhaes, D. Chasseau, and C. Hauw, *Solid State Commun.* **52**, 177 (1984).
- ²⁴T. Mori, A. Kobayashi, Y. Sasaki, H. Kobayashi, G. Saito, and H. Inokuchi, *Chem. Lett.*, 957 (1984).
- ²⁵P. C. W. Leung, T. J. Emge, A. J. Schultz, M. A. Beno, K. D. Carlson, H. H. Wang, M. A. Firestone, and J. M. Williams, *Solid State Commun.* **57**, 93 (1986).
- ²⁶T. Sugano, G. Saito, and M. Kinoshita (unpublished).
- ²⁷E. B. Yagubskii, I. F. Shchegolev, R. P. Shibaeva, D. N. Fedutin, L. P. Rozenberg, E. M. Sogomonyan, R. M. Lobkovskaya, V. N. Laukhin, A. A. Ignat'ev, A. V. Zvarykina, and L. I. Buravov, *Pis'ma Zh. Eksp. Teor. Fiz.* **42**, 167 (1985).
- ²⁸F. J. Dyson, *Phys. Rev.* **98**, 349 (1955).
- ²⁹M. Tokumoto, H. Bando, H. Anzai, G. Saito, K. Murata, K. Kajimura, and T. Ishiguro, *J. Phys. Soc. Jpn.* **54**, 869 (1985).
- ³⁰H. J. Pedersen, J. C. Scott, and K. Bechgaard, *Phys. Rev. B* **24**, 5014 (1981).
- ³¹K. Mortensen, J. M. Williams, and H. H. Wang, *Solid State Commun.* **56**, 105 (1985).
- ³²V. A. Merzanov, E. E. Kostyuchenko, O. E. Faber, I. F. Shchegolev, and E. B. Yagubskii, *Zh. Eksp. Teor. Fiz.* **89**, 292 (1985).
- ³³In this work, we refer to the crystal data given in Ref. 22. Note that the *a* and *b* axes in the work done by Merzhanov *et al.* correspond, respectively, to the *b* and *a* axes in Ref. 22.
- ³⁴C. S. Jacobsen, J. M. Williams, and H. H. Wang, *Solid State Commun.* **54**, 937 (1985).
- ³⁵G. Feher and A. F. Kip, *Phys. Rev.* **98**, 337 (1955).
- ³⁶Y. Yafet, in *Solid State Physics*, edited by H. Ehrenreich, F. Seitz, and D. Turnbull (Academic, New York, 1963), Vol. 14, p. 1.
- ³⁷Evidence for a structural transition has been suggested by H. Schwenk, F. Gross, C.-P. Heidmann, K. Andres, D. Schweitzer, and H. Keller, *Mol. Cryst. Liq. Cryst.* **119**, 329 (1985). They suggest that the transition does not take place at the sites of the BEDT-TTF molecule and speculate on the possibility of orientational ordering due to the distortion of the triiodide anion.
- ³⁸T. Sugano and H. Kuroda, *Chem. Phys. Lett.* **47**, 92 (1977).